

A Low-Profile Reconfigurable Wide Band BPF with RF-MEMS Switches for 5G/Satellite Applications

Surendra Babu Velagaleti

Department of ECE, KLEF, Vaddeswaram, Guntur, Andhra Pradesh, India | Department of ECE, C. R. Reddy Engineering College, Eluru, India
vsb.mtech14@gmail.com (corresponding author)

Siddaiah Nalluri

Department of ECE, KLEF, Vaddeswaram, Guntur, Andhra Pradesh, India
siddaiah@kluniversity.in

Received: 2 October 2024 | Revised: 14 October 2024 | Accepted: 22 October 2024

Licensed under a CC-BY 4.0 license | Copyright (c) by the authors | DOI: <https://doi.org/10.48084/etasr.9159>

ABSTRACT

A low-profile wide-band tunable semi-circular cavity BPF is designed and analyzed in this work. RF-MEMS switches were utilized on either side of the 50Ω microstrip transmission lines to provide reconfigurability. BPF tunability is achieved when the two switches travel from upstate to downstate in an electrostatically activated shunt capacitive shunt type RF-MEMS switch. The switch has a capacitance ratio of 10 and operates at a transition time of $30 \mu\text{s}$ with an actuation voltage of 6.5 V to move it downward. This is suitable for 5G wireless communication applications (n77, n78, and n79) as well as C-band applications. Return loss of -22 dB is obtained at 3.7 GHz when the switch is in the ON state, while reflection co-efficient of -32 dB is obtained at 6.7 GHz when the switch is in the OFF state. When both switches are ON or OFF, a bandpass filter provides a 3GHz frequency shift. The frequency range where BPF is intended to operate, which is adjustable for various purposes, is 1–10 GHz. The characteristics of the switch were investigated by simulating its design in COMSOL Multiphysics and the outcomes were contrasted with theoretical computations. The adjustable properties of the BPF have been observed and shown using the HFSS v 13 tool.

Keywords-5G applications; semi-circular cavity; satellite communication applications; return loss; insertion loss; transition time

I. INTRODUCTION

Communication technologies have changed significantly in the last years. Analog transmission has long been a feature of conventional distribution systems, such as satellite broadcasts, radio relays, and cables. However, they have, drastically changed/transformed into digital broadcasting in recent times. Many countries around the world have already employed digital broadcasting via satellite. The market for small, incredibly efficient, and reasonably affordable microwave systems and equipment has grown because of these improvements, which have also increased bandwidth requirements and raised microwave frequency bands. Another essential component of modern telecommunications systems is their ability to reorganize themselves to meet new requirements. One such example of a reconfigurable system is a Software-Defined Radio (SDR) [1, 2]. In such circumstances, filters are crucial since they are a necessary component of almost all communication systems. There is a plethora of knowledge on traditional filter design methods and circuitry in

the literature [3, 4]. Then, to make the same RF front-end reusable, it dynamically modified its mode of operations to satisfy the needs and specifications of the application. Electrically controlled tunable bandpass filters will play a critical role in future multi-standard, multifunction wireless communication systems due to their compact size and ability to function on several frequency bands. Planar microstrip filters are the chosen option due to their low cost and simple fabrication procedures. Planar microstrip resonator filters come in a variety of forms [10], including resonators, open loop resonators, and stepped impedance resonator filters, all of which have been effectively applied for a range of uses [11–14]. Reconfigurability, however, is a major trend in microwave or radio frequency systems, particularly in the current market. The same RF front end dynamically changed its mode of operation to meet the requirements and application standards in order to make be reusable. Specifically, due to their small design and flexibility to operate on several frequency bands, electronically controlled reconfigurable bandpass filters will be crucial in future multi standard, multifunction wireless

communication systems. Therefore, reconfigurable bandpass filters can lower costs and adjust to regulatory changes by accommodating multiple standards' bandwidth needs [15–18]. By altering the inter-resonator couplings, filters can have different properties and bandwidths. This technique is simply applied to coupled line filters, in which the lengths and distances of the overlapping sections are the only factors determining the coupling between the elements. Specifically, electronic switching devices make it simple to adjust the length of coupling sections. For linked lines filters, hairpin bandpass filters are favored due to their compactness [19, 20]. A folded half-wave parallel-coupled filter is called a hairpin bandpass filter. Specifically, hairpin filters are created by folding the resonator ends back into a "U" shape after starting with a parallel-coupled filter; this technique dramatically lowers the resonator's size and quality factor Q [21]. Similar to linked line filters, hairpin constructions can be adjusted by adding a section of microstrip lines with appropriate electronic switches and changing the length of the resonators. This is because electronic switches need driving circuitry, which can lower the Q-factor of the filter's elements. Reconfigurable filters have also made extensive use of PIN diodes as electrical switches. They are not the ideal option, though, as the driving circuitry can significantly lower the quality factor Q and they need large currents to function well [22, 23].

This article describes the design and integration of a shunt capacitive RF MEMS switch that is electrostatically operated in order to lower the pull-in potential. For satellite communication applications as well as 5G applications (n77, n78, and n79), a reconfigurable BPF with an RF-MEMS switch is designed and evaluated. Parameters like as actuation voltage, switching time, operating frequency, isolation and insertion losses are used to assess the performance of switches. In order to assess the reconfigurability of return loss and insertion loss for 5G wireless communication applications, the suggested switch is combined with the BPF.

II. DESIGN ANALYSIS

Two components make up the proposed design: an RF MEMS switch and a semi-circular cavity-based BPF. For use in 5.8 GHz–7.8 GHz satellite communication applications as well as 3 GHz–5.4 GHz 5G applications, a reconfigurable semi-circular cavity based BPF with an integrated RF MEMS switch is utilized. The effectiveness of the BPF is unaffected by employing two switches on either side of the feed lines because the suggested shunt capacitive switch is intended to operate at two distinct bands.

A. Analysis of Shunt Capacitive RF-MEMS Switch

The BPF's reconfigurability is examined using an RF-MEMS shunt capacitive switch, and it is implemented deploying a 50 Ω transmission line. Figure 1 shows the dimensions of the RF MEMS capacitive switch, which are 400 μm × 200 μm length and width, respectively. Table I depicts the RF-MEMS switch's parameters. There are two modes of operation for RF-MEMS switches: ON and OFF. The actuation voltage is applied to the beam to activate the RF MEMS switch. The lower electrode and the switch come into electrical contact when the switch is triggered. Electromechanical

performance metrics, such as the time it takes to switch from an ON to an OFF state, the actuation voltage, and lumped element parameters, like capacitance, inductance, and resistance, are used to assess switch membranes. The RF-MEMS switch was designed with a beam thickness of 1 μm and a dielectric thickness of 0.3 μm.

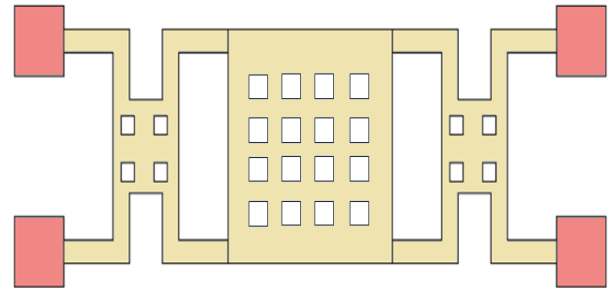


Fig. 1. Shunt capacitive RF-MEMS switch.

TABLE I. FEATURES OF SHUNT CAPACITIVE RF-MEMS SWITCH

Parameter	Value	Parameter	Value
Length	400 μm	Conduct area	100 μm ² ×100 μm ²
Width	200 μm	Actuation voltage	6.5V
height	1.6 μm	switching time	30 μS
Type	bridge	Insertion	0.1712 dB
Gap	3 μm	Isolation	50 dB
Holes	8×8	Downstate Capacitance	4.74×10 ⁻¹²

For the proposed shunt capacitive switch, the simulated frequency response and impedance matching are examined. The mathematical formulas that were employed while developing the switch are provided below. To control the voltage from the signal line, lumped RLC components must be considered prior to determining the RF parameters of the switch. The following equations provide a detailed explanation of the operation mechanism, which is dependent on the lumped RLC components. By using these equations, one may determine the parameters of the RF switch:

$$L = 0.002l \left(\ln \frac{2l}{w+t} + 0.50049 + \frac{w-t}{3l} \right) \tag{1}$$

$$R = \rho \frac{L}{S} \tag{2}$$

$$c_u \approx \epsilon_0 \frac{A}{g}, c_d = \epsilon_0 \cdot \epsilon_r \frac{A}{t_d} \tag{3}$$

$$f = \frac{1}{2\pi} \sqrt{\frac{k}{m}} \tag{4}$$

$$t_s = 3.67 \frac{V_p}{V_s} \sqrt{\frac{m}{k}} \tag{5}$$

where m is the beam's mass, Vs is the switch voltage, and Vp is the pull voltage. K is the spring constant. Figure 2 portrays the equivalent circuit of the RF-MEMS shunt capacitive switch in terms of the lumped parameters.

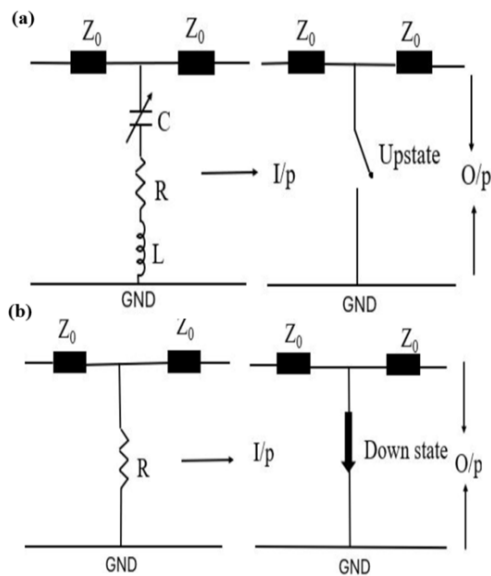


Fig. 2. Shunt capacitive RF-MEMS switch equivalent circuit (a) ON state, (b) OFF state.

Lumped elements are employed to assess the device's RF performance. It is critical to consider the typical values of these elements, particularly the capacitance values in the switch's ON and OFF states, as seen in the equivalent circuit.

B. Analysis of RF-Wideband BPF

The thickness of the FR4 epoxy material employed in the proposed tunable BPF is 1.6 mm, with an ϵ_r of 4.4 and a δ of 0.02. The reconfigurable BPF occupies an area of $40 \text{ mm}^3 \times 40 \text{ mm}^3 \times 1.6 \text{ mm}^3$. A trapezoidal pattern is obtained by subtracting two circles from each of the two circular rings. A circular slot is added to the trapezoidal section of the filter. Semicircular cavity filters are used in communication equipment to either accept or reject frequencies. The iteration-orientated design of a tunable BPF is presented in Figure 3.

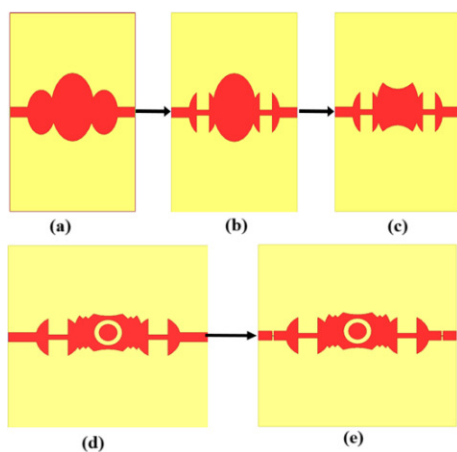


Fig. 3. Development of the reconfigurable BPF: (a) initial iteration, (b) second iteration, (c) third iteration, (d) fourth iteration, (e) fifth iteration.

TABLE II. GEOMETRIC PARAMETERS OF THE RECONFIGURABLE BPF

Parameter	Values (mm)
L1	40
W1	40
L2	7.9
W2	16
L3	2
W3	4
W4	5.8
W5	5.64
W6	1

Three circular rings are attached to the transmission line at the first stage. Step 2 involves etching two rectangular strips from the circular rings to obtain a semicircular cavity on both sides of the filter. The step 3 filter is generated by deducting two circular rings from the core circular resonator. The fourth step entails etching a diagonal square from the main circular stub's four ends. Moreover, a circular slot is etched from the primary stub. Step 5 includes etching the last two diagonal square stubs from the main stub. In wireless communication, the bandpass filter's major goals are to improve selectivity and reduce insertion loss while separating frequency bands and isolating channels. The signal-to-noise ratio is increased by using BPFs to filter out unwanted frequencies, which enhances the overall quality of both sent and received signals.

C. Tunable BPF with Shunt Capacitive RF-MEMS Switch

Figure 4 illustrates a wide-band BPF that incorporates a MEMS switch. The previous section covered the BPF and RF-MEMS switch specifications. Satellite communication applications and 5G applications (n77, n78, and n79) use reconfigurable semi-circular cavity BPF. The BPF resonates at the targeted frequency bands when the switch is in the ON or OFF position. This results in the reconfiguration of return loss, insertion loss, and group delay. The RF-MEMS switches regulate how the BPF is tuned. Two MEMS switches were used in this paper to improve the BPF's performance. Table IV displays the impedance bandwidths and resonance frequencies. Switch actuates towards the electrode when the ON condition is present, and the BPF resonates at 3.7 GHz with a 2.4 GHz bandwidth, making it suitable for 5G- Sub-6 GHz applications. BPF resonates at 6.7 GHz with a bandwidth of 2 GHz when it is in the OFF state. The reconfigurable BPF and RF MEMS switch must first have its parameters optimized using mathematical techniques before analysis can begin. Subsequently, electromagnetic techniques are used for simulation assessments, allowing for the evaluation of the individual and combined behaviors of both components. After the simulation, BPF undergoes a methodical performance assessment to verify its functionality. A close examination is conducted of performance factors such as group delay, insertion loss, and return loss. Similar to this, a thorough assessment of the RF MEMS switch is carried out to validate its functionality, performance parameters, switching time, and dependability. This integration method ensures good compatibility and operation between the switch and the filter.

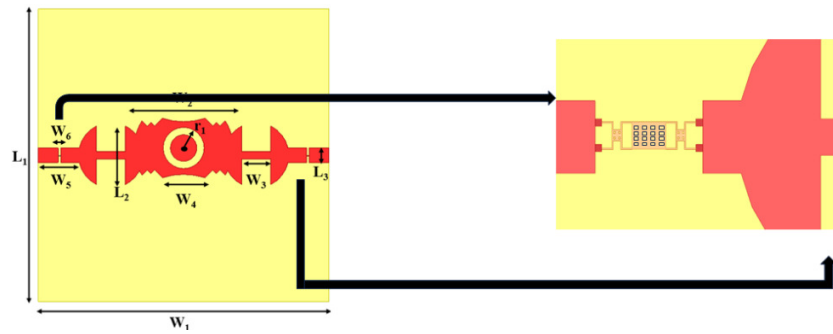


Fig. 4. Tunable BPF with RF-MEMS switches.

TABLE III. VARIOUS SWITCHING WITH RF-MEMS SWITCHES

Operation States	S ₁	S ₂	Center Frequency	Bandwidth
State 1	OFF	OFF	6.7GHz	2GHz
State 2	OFF	ON	-----	-----
State 3	ON	OFF	-----	-----
State 4	ON	ON	3.7GHz	2.4 GHz

III. RESULTS AND DISCUSSION

An-soft HFSS is used for the bandpass filter's RF analysis. S-parameters and group delay are the two most crucial parameters that need to be assessed for any RF device throughout a broad frequency range. The switch is in the ON state when there is no voltage supplied across the beam. Within the frequency range of 1 GHz – 10 GHz, the insertion and return losses of an ON-state switch with a silicon nitride dielectric layer spaced two millimeters apart are determined. When the switch senses an actuation voltage, it goes into an OFF state and the signal stays in the same condition. The beam collapsing into the dielectric layer above the signal line is the source of this. Figure 5 shows the reconfigurable BPF's reflection coefficient when both switches are in the ON/OFF position. The reconfigurable BPF resonates at 6.7 GHz and fits the requirements of 5G applications n77 (3300–4200 MHz), n78 (3300–3800 MHz), and n79 (4400–5000 MHz) when both switches are switched ON. The reconfigurable BPF resonates at 3.7 GHz when both switches are turned ON, meeting the requirements of 5G- Sub-6 GHz applications. The tunable BPF resonates at 3.7 GHz and 5.2 GHz and provides an impedance bandwidth of 2.4 GHz, return loss of -15dB and -22dB, and insertion loss of -1.5dB and -2dB when the switch is in the ON position. Figure 5 also shows the reconfigurable BPF's transmission coefficient. At both resonant frequencies, the transmission coefficient is less than 3dB and the return loss is less than -10dB. When the switch is in the OFF position, the reconfigurable BPF resonates at 6.7 GHz with an impedance bandwidth of 2 GHz, a reflection coefficient of -37dB, and a transmission coefficient of -2dB. It is therefore suitable for applications involving satellite communication. Since the primary factor influencing the reconfigurability of the filter is the capacitance of the switches, the resonant frequency can be adjusted as the switches transition from an up state to a down state, increasing their capacitance. The BPF's resonant frequency shifts as a result of the two capacitances being in parallel, raising the total capacitance. There is a 3 GHz frequency shift when both switches are turned on. Figure 6

shows the time domain properties of the tunable BPF, which are computed using the group delay. A set of delays of 2nS is provided by the filter's delay, which causes minimal signal distortion.

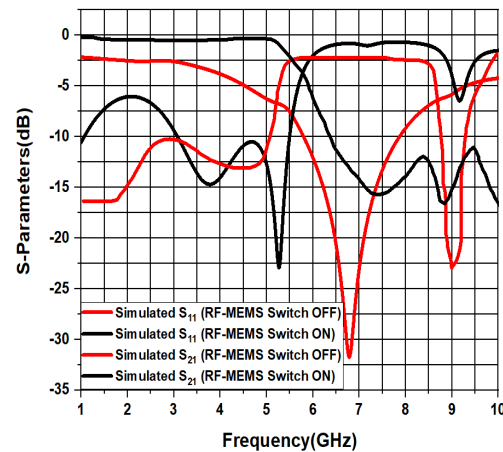


Fig. 5. S-parameters of the Tunable BPF.

The spring's mechanical suspension is determined by the force applied to it, as per the damper system [23]:

$$F = K \cdot X \tag{6}$$

$$K = F/X \tag{7}$$

As a result, the beam is forced, its displacement is calculated, and the resulting ratio provides the value of the simulated spring constant. A force of 1 μN is delivered to the beam, and the switch shifts 0.02 μN in the Z-axis direction at 1 μN. The displacement of the beam caused by force application using the FEM tool is shown in Figure 7. The capacitive RF MEMS switch performance can be improved by decreasing the upstate capacitance and increasing the downstate capacitance. The material used as a dielectric between the membrane and bottom electrode primarily controls capacitance variation. The upstate capacitance of the proposed switch accounts for the tiny fringing field capacitance brought on by the perforation. The term "up-state capacitance" refers to the capacitance that the switch acquires when it is turned on. Table IV presents the comparison of the reconfigurable BPF with the available reconfigurable bandpass filters. The proposed BPF offers better results in terms of return loss, insertion loss, and group delay and it even occupies less space.

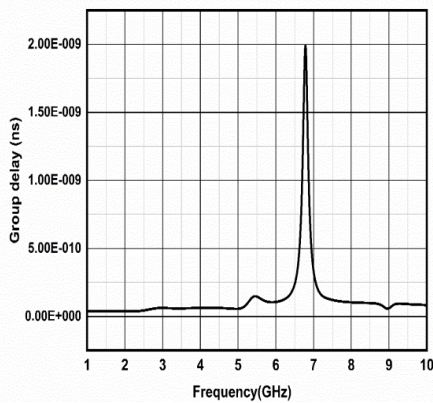


Fig. 6. Group delay of the reconfigurable BPF.

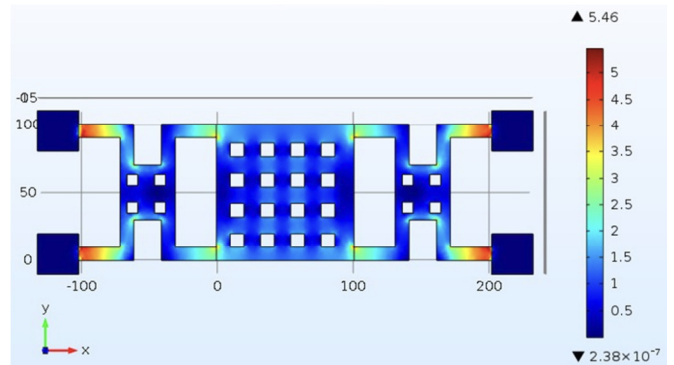


Fig. 7. Displacement analysis of shunt capacitive RF-MEMS switch.

TABLE IV. COMPARISON OF THE RECONFIGURABLE BPF WITH THE OTHER BPF'S

References	F (GHz)	FBW	IL (dB)	RL (dB)	Group delay (nS)	Size (λg ²)
[1]	3.5/5.24	-	1.5/1.6	12/13	-	1.4×1.4
[2]	2.55/3.65	6.72/5.45	1.2/2	19/19	0.9	0.89×0.89
[3]	2.49/3.50	15.60/8	1.22/1.22	13/13	0.4	0.87×0.87
[4]	2.53/5.76	4/3	1.3/1.4	15/14	0.963	1.5×1.7
[5]	2/4	5.5/4	1.22/1.23	17/17	0.879	1.2×1.32
[6]	2.4/3.8	12/10	2/1	18/19	0.756	0.87×0.87
[7]	2.5/1.3	2/0.9	0.99/0.55	17/19	0.854	0.68×0.68
[8]	2.5/5.6	-	0.58/1.8	16/15	-	0.258×0.258
[9]	2.1/2.6	1.4/2.1	1.9/1.63	15/19	0.778	0.798×0.798
This study	3.7, 5.2/6.7	2.4/2	-1.5, -2/-2	-22/-32	2/2	0.188×0.188

IV. CONCLUSIONS

This paper presents the novel design and analysis of an RF-MEMS switch loaded on a semi-circular cavity BPF. A high degree of agreement between the simulated and calculated results confirms the effectiveness of the proposed RF-MEMS switch design, which is used to improve a BPF's reconfigurability features. The frequency of the BPF was adjusted by raising the capacitance value by connecting the two switches in parallel. Return loss of -22 dB is obtained at 3.7 GHz when the switch is in the ON state, while a reflection coefficient of -32 dB is obtained at 6.7 GHz when the switch is in the OFF state. When the switch is in the ON state, the return loss is measured at 3.7GHz, and when it is in the OFF state, it is measured at 6.7 GHz. This is appropriate for satellite communication applications as well as 5G wireless communication applications (n77, n78, and n79). A 3 GHz frequency shift is obtained when one or both switches are in the ON (or OFF) position. The switch is designed and implemented to raise the tunability quality of the BPF, featuring a short group latency of 2nS, a fast-switching speed of 30 μS, a high capacitance ratio of 10, and a low pull-in voltage of 6.5 V.

REFERENCES

[1] S. Nam, M. Z. Koohi, W. Peng, and A. Mortazawi, "A Switchless Quad Band Filter Bank Based on Ferroelectric BST FBARs," *IEEE Microwave and Wireless Components Letters*, vol. 31, no. 6, pp. 662–665, Jun. 2021, <https://doi.org/10.1109/LMWC.2021.3069880>.
 [2] G. B. and R. R. Mansour, "A Tunable Quarter-Wavelength Coaxial Filter With Constant Absolute Bandwidth Using a Single Tuning

Element," *IEEE Microwave and Wireless Components Letters*, vol. 31, no. 6, pp. 658–661, Jun. 2021, <https://doi.org/10.1109/LMWC.2021.3064381>.
 [3] A. Fernández-Prieto, J. Naqui, J. Martel, F. Martín, and F. Medina, "Coupled-Resonator Balanced Bandpass Filters with Common-Mode Suppression Differential Lines," in *Balanced Microwave Filters*, John Wiley & Sons, Ltd, 2018, pp. 73–89.
 [4] G. Immadi, N. K. Majji, M. V. Narayana, and A. Navya, "Comparative Analysis of Pass Band Characteristics of a Rectangular Waveguide with and Without a Dielectric Slab," *International Journal of Innovative Technology and Exploring Engineering*, vol. 8, no. 6, 2019.
 [5] G. Immadi, M. V. Narayana, A. Navya, Y. D. S. Sairam, and K. Shrimanth, "Design and Analysis of Micro strip Circular Ring Band Stop Filter," *International Journal of Innovative Technology and Exploring Engineering*, vol. 8, no. 4, 2019.
 [6] S. Yang, W. Li, M. Vaseem, and A. Shamim, "Additively Manufactured Dual-Mode Reconfigurable Filter Employing VO₂-Based Switches," *IEEE Transactions on Components, Packaging and Manufacturing Technology*, vol. 10, no. 10, pp. 1738–1744, Jul. 2020, <https://doi.org/10.1109/TCPMT.2020.3019067>.
 [7] A. Navya, G. Immadi, and M. V. Narayana, "A Low-Profile Wideband BPF for Ku Band Applications," *Progress In Electromagnetics Research Letters*, vol. 100, pp. 127–135, 2021, <https://doi.org/10.2528/PIERL21082101>.
 [8] X.-K. Zhang, X.-Y. Wang, S.-C. Tang, J.-X. Chen, and Y.-J. Yang, "A Wideband Filtering Dielectric Patch Antenna With Reconfigurable Bandwidth Using Dual-Slot Feeding Scheme," *IEEE Access*, vol. 9, pp. 96345–96352, 2021, <https://doi.org/10.1109/ACCESS.2021.3095080>.
 [9] D.-S. Wu, Y. C. Li, Q. Xue, and B.-J. Hu, "Balanced Dielectric Resonator Filters With Multiple Reconfigurable Passbands," *IEEE Transactions on Microwave Theory and Techniques*, vol. 70, no. 1, pp. 180–189, Jan. 2022, <https://doi.org/10.1109/TMTT.2021.3081989>.
 [10] A. Navya, G. Immadi, and M. V. Narayana, "Design and Analysis of a Compact Wide-Band BPF using Quarter Wave Transmission Lines,"

- Journal of Engineering Science and Technology Review*, vol. 15, no. 4, pp. 33–36, 2022, <https://doi.org/10.25103/jestr.154.05>.
- [11] Ambati, Navya, Govardhani, Immadi, Madhavareddy, Venkata Narayana, and Department of ECE, KLEF, Vaddeswaram, Guntur, Andhra Pradesh, India, "Flexible ku/k band frequency reconfigurable bandpass filter," *AIMS Electronics and Electrical Engineering*, vol. 6, no. 1, pp. 16–28, 2022, <https://doi.org/10.3934/electreng.2022002>.
- [12] M. Houssini, A. Pothier, A. Crunteanu, and P. Blondy, "A 2-pole digitally tunable filter using local one bit varactors," in *2008 IEEE MTT-S International Microwave Symposium Digest*, Jun. 2008, pp. 37–40, <https://doi.org/10.1109/MWSYM.2008.4633097>.
- [13] A. Kaiser, "The potential of MEMS components for re-configurable RF interfaces in mobile communication terminals," in *Proceedings of the 27th European Solid-State Circuits Conference*, Sep. 2001, pp. 25–28.
- [14] G. M. Rebeiz, *RF MEMS: Theory, Design, and Technology*. John Wiley & Sons, 2004.
- [15] A. Navya, G. Immadi, M. V. Narayana, and A. S. Madhuri, "Design and Analysis of a Quad Band BPF Using Ring Resonator," in *2023 7th International Conference on Computation System and Information Technology for Sustainable Solutions (CSITSS)*, Aug. 2023, pp. 1–4, <https://doi.org/10.1109/CSITSS60515.2023.10334134>.
- [16] A. Ocera, P. Farinelli, P. Mezzanotte, R. Sorrentino, B. Margesin, and F. Giacomozzi, "A Novel MEMS-Tunable Hairpin Line Filter on Silicon Substrate," in *2006 European Microwave Conference*, Sep. 2006, pp. 803–806, <https://doi.org/10.1109/EUMC.2006.281041>.
- [17] J. Iannacci, D. Masotti, T. Kuenzig, and M. Niessner, "A reconfigurable impedance matching network entirely manufactured in RF-MEMS technology," in *Smart Sensors, Actuators, and MEMS V*, May 2011, vol. 8066, pp. 280–291, <https://doi.org/10.1117/12.886186>.
- [18] J. Iannacci, M. Huhn, C. Tschoban, and H. Pötter, "RF-MEMS Technology for 5G: Series and Shunt Attenuator Modules Demonstrated up to 110 GHz," *IEEE Electron Device Letters*, vol. 37, no. 10, pp. 1336–1339, Jul. 2016, <https://doi.org/10.1109/LED.2016.2604426>.
- [19] J. Iannacci, M. Huhn, C. Tschoban, and H. Pötter, "RF-MEMS Technology for Future Mobile and High-Frequency Applications: Reconfigurable 8-Bit Power Attenuator Tested up to 110 GHz," *IEEE Electron Device Letters*, vol. 37, no. 12, pp. 1646–1649, Sep. 2016, <https://doi.org/10.1109/LED.2016.2623328>.
- [20] N. Ambati, G. Immadi, M. V. Narayana, K. R. Bareddy, M. S. Prapura, and J. Yanapu, "Parametric Analysis of the Defected Ground Structure-Based Hairpin Band Pass Filter for VSAT System on Chip Applications," *Engineering, Technology & Applied Science Research*, vol. 11, no. 6, pp. 7892–7896, Dec. 2021, <https://doi.org/10.48084/etasr.4495>.
- [21] N. K. Majji, V. N. Madhavareddy, G. Immadi, N. Ambati, and S. M. Aovuthu, "Analysis of a Compact Electrically Small Antenna with SRR for RFID Applications," *Engineering, Technology & Applied Science Research*, vol. 14, no. 1, pp. 12457–12463, Feb. 2024, <https://doi.org/10.48084/etasr.6418>.
- [22] N. K. Majji, V. N. Madhavareddy, G. Immadi, and N. Ambati, "A Low-Profile Electrically Small Serrated Rectangular Patch Antenna for RFID Applications," *Engineering, Technology & Applied Science Research*, vol. 14, no. 2, pp. 13611–13616, Apr. 2024, <https://doi.org/10.48084/etasr.6989>.
- [23] R. Marcelli, A. Lucibello, G. De Angelis, E. Proietti, and D. Comastri, "Mechanical modelling of capacitive RF MEMS shunt switches," *Microsystem Technologies*, vol. 16, no. 7, pp. 1057–1064, Jul. 2010, <https://doi.org/10.1007/s00542-009-1007-y>.